Bull. Disas. Prev. Res. Inst., Kyoto Univ., Vol. 45, Part 2,3 No. 391, February, 1996

A Simple Water Balance Model for a Mesoscale Catchment Based on Heterogeneous Soil Water Storage Capacity

By Nirupama, Yasuto TACHIKAWA, Michiharu SHIIBA and Takuma TAKASAO

(Manuscript received on Aug. 25, 1995, revised on Feb. 8, 1996)

Abstract

The work presented in this paper has been motivated by the need to develop a simple parameterization method for rainfall-runoff modelling considering spatial heterogeneity. A concept of tension water storage capacity distribution has been incorporated into a rainfall-runoff model to explain the runoff generation phenomenon more realistically. Originally, the concept was initiated by Zhao *et al.* (1980) in the Xinanjiang model, and later adopted by many researchers, e.g., in the VIC model by Wood *et al.* (1992). However, the expression for the tension water storage distribution in the Xinanjiang model is unable to describe all the situations in natural catchments. We therefore propose a general expression for the tension water storage capacity distribution. Applying this general expression, we have compared the performances of four kinds of rainfall-runoff simulation models, which are, the VIC model (Model 1), the unconfined version of VIC model (Model 2), and two models with a different concept of runoff generation mechanism with confined (Model 3) and unconfined (Model 4) aquifer cases, for the mesoscale catchments of Japan and Thailand.

Sensitivity analysis of the model parameters has been conducted as well. The effect of time and spatial scale is also brought out. As a result, we can say that Model 3 and Model 4 indicate better runoff estimation and realistic soil-water storage time series, whereas, Model 1 and Model 2 are not able to represent a realistic time series of soil-water storage.

1. Introduction

Water plays a fundamental role in the redistribution of solar energy through the energy associated with evapotranspiration, the transport of atmospheric water vapor and precipitation. Hydrologists the world over are now aware of the fact that a simple bucket concept does not explain the actual phenomenon of rainfall-runoff process and evaporation. Catchments are spatially heterogeneous in terms of vegetation, soil wetness and sub-surface processes like runoff generation.

A first attempt to better represent the rainfall-runoff modelling through a concept of tension water storage distribution was made in the Xinanjiang model by Zhao *et al.* (1980), which is becoming acceptable to more and more scientists. To cite a few, Wood *et al.* (1992) in the VIC model, and Dümenil and Todini (1992) in the Arno scheme, have adopted a similar concept for a saturation-excess mechanism for surface runoff generation, with reduction in the number of paramaters. Additionally, Lu *et al.* (1995) worked on the Xinanjiang model and explained its performance using the Priestley-Taylor method for evapotranspiration values. Recently, Sivapalan and Woods (1995)

and Kalma *et al.* (1995) also have adopted the theory of spatially distributed soil moisture in their research.

Although, the Xinanjiang model performs well for the Chinese catchments, it suits only the daily discharge simulation for the Japanese river catchment (Nirupama *et al.*, 1995). The spatial distribution representing the soil water storage capacity used in the Xinanjiang model is of inflexible nature and could be generalized to improve the runoff simulation process, as proposed in this paper. Using the proposed general expression for the tension water storage capacity distribution, a rainfall-runoff model, considering tension water storage variation and confined or unconfined aquifer condition, is proposed. The applicability of the models has been checked on the Kizu River basin in Japan and the Ping River basin in Thailand.

2. Methodology

2.1 Motivation for proposing general expression for the tension water storage capacity distribution

The concept of spatial distribution of tension water storage capacity proposed in the Xinanjiang model is shown in Fig. 1, where f is pervious and F total area of the sub-basin, $W'M$ is tension water capacity within the sub-basin, MM is the maximum value of $W'M$. IM is the fraction of impervious area, R is runoff, P is the precipitaion, K is the ratio of potential evaporation to pan evaporation EM, and W is spatial mean tension water storage. The tension water storage distribution is expressed by the following equation

$$W'M=MM\left[1-\left(1-\frac{\frac{f}{F}-IM}{1-IM}\right)^{\frac{1}{b}}\right] \quad , IM<\frac{f}{F}\leq 1 \tag{1}$$

where b is a parameter, and $W'M=0$ when $0\leq f/F\leq IM$. Integration of Equation (1) w.r.t. f/F, with limits 0 to 1, shows that

$$MM=WM\frac{(1+b)}{(1-IM)} \tag{2}$$

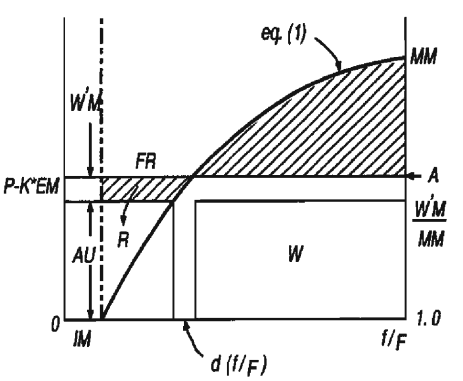

Fig. 1. The Xinanjiang Model Concept.

where WM is maximam water storage capacity. The relationship between MM and WM is related through the parameter b. However, this relationship is unable to describe all the situations in natural catchments for the following reasons:

1. Soil tension water capacity (STWC) within the basin varies between zero and some maximum value, MM. However, this is not always valid. Specifically, in natural catchments all points of a basin might have STWC of more than 0 with the minimum STWC being much greater than zero, as can be seen in Fig. 2(a).
2. In natural catchments it is possible that $W'M$ becomes the same as the maximum value, MM, for certain fractions of the pervious area of the basin as shown in Fig. 2(b). Under such a condition, it is desirable to use a distribution function which takes care of this situation.
3. There may be two different catchments having the same spatial average STWC but with different distribution functions (see Fig. 2(c)) due to different soil characteristics of these catchments, which can not be described by Zhao.

Thereby, we propose the general expression for tension water storage capacity distribution.

2.2 Proposed distribution function

In the proposed modified expression given below, by adding only one parameter, m, the various soil water storage situations in natural catchments can be taken care of.

$$W'M=\begin{cases} MM\left[1-\left(1-\dfrac{\dfrac{f}{F}-IM}{1-IM}\right)^{\frac{1}{b}}\right]^{m-1} & \text{if} \quad IM<\dfrac{f}{F}\leq 1 \\ 0 & \text{if} \quad 0\leq\dfrac{f}{F}\leq IM \end{cases} \tag{3}$$

Here the meaning of the variables is the same as in Equation (1). Note that when m is equal to 2, Equation (3) reduces to Equation (1), which is explained by Zhao.

Interestingly, when m is equal to 1, then $W'M/MM$ becomes 1 at all the f/F values, which means that at m equal to 1, Equation (3) describes the bucket model. And also, if we let m approach infinity, $W'M/MM$ tends to 0 because the term $(1-f/F)^{\frac{1}{b}}$ will always be less than 1. Thus, Equation (3) can describe the above stated extreme cases, e.g., (a)

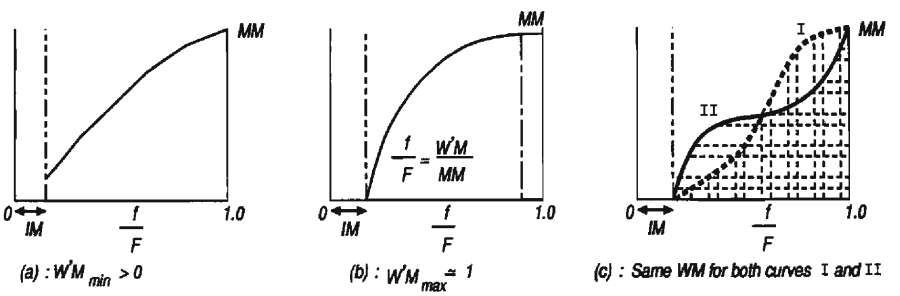

Fig. 2. The three Different Cases of STWC Distribution Function.

uniform STWC, i.e., uniformly fully saturated conditions and (b) impervious basin, i.e., insignificant STWC.

Let us obtain the relationship between WM and MM. Refering to Fig. 1,

$$WM=\int_0^1 W'M\, d\left(\frac{f}{F}\right)$$

$$=\int_{IM}^1 \mathrm{MM}\left[1-\left(1-\frac{\frac{f}{F}-IM}{1-IM}\right)^{\frac{1}{b}}\right]^{m-1} d\left(\frac{f}{F}\right) \tag{4}$$

Let $\dfrac{\frac{f}{F}-IM}{1-IM}=y$ and hence $d\left(\frac{f}{F}\right)=(1-IM)\,dy$. Equation (4) can be written as

$$WM=(1-IM)\,\mathrm{MM}\int_0^1 [1-(1-y)^{\frac{1}{b}}]^{m-1}dy \tag{5}$$

let, $1-(1-y)^{\frac{1}{b}}=z$, now Equation (5) can be written as,

$$WM=b(1-IM)\,\mathrm{MM}\int_0^1 z^{m-1}(1-z)^{b-1}dz \tag{6}$$

Note that $\int_0^1 z^{m-1}(1-z)^{b-1}dz$, when $m>0$, $b>0$, is nothing but the complete Beta function which is related to the Gamma function as follows:

$$\mathrm{B}(m,\ b)=\frac{\Gamma(m)\Gamma(b)}{\Gamma(m+b)} \tag{7}$$

substituting Equation (7) in Equation (6)

$$WM=\frac{\Gamma(m)\Gamma(b+1)}{\Gamma(m+b)}(1-IM)\cdot \mathrm{MM} \tag{8}$$

This means that the spatial mean tension water capacity is related to Gamma function as

$$MM=WM\frac{\Gamma(m+b)}{\Gamma(m)\Gamma(b+1)}\frac{1}{(1-IM)} \tag{9}$$

When $m=2$, Equation (9) reduces to Equation (2) in the Xinanjiang model.

2.3 Water Balance Models Based on Heterogeneons Soil Water Storage Capacity

Using the general expression for spatial tension water storage capacity distribution, we compared the performances of four kinds of rainfall-runoff simulation models, e.g., the VIC model (Model 1), unconfined version of VIC model (Model 2), and two models with a different concept of runoff generation mechanism with confined (Model 3) and unconfined (Model 4) aquifer cases.

In Model 1, runoff generation at a point happens when the soil reaches it's water storage capacity at that point (Fig. 3). In the event of precipitation there is an increase in the saturated area, from *abc* to *ab'c'*, resulting in an increase in groundwater storage. Subsurface runoff is taken as a function of the soil moisture storage W. The variation in storage capacity i over a basin could be defined as

$$i=\begin{cases}0 & \text{if} \quad 0\le A\le A_i\\ i_m\left[1-\left(1-\dfrac{A-A_i}{1-A_i}\right)^{1/b}\right] & \text{if} \quad A_i<A\le 1.0\end{cases} \tag{10}$$

where i_m is the point maximum tension water capacity, A is the fraction of the basin area which takes values between 0 and 1, and b is an empirical parameter. A_i is the impervious portion of the basin. From the impervious area, the runoff depth Q_i occurs which is represented as

$$Q_i = A_i (P-E) \tag{11}$$

From the pervious area runoff depth Q_p is given by

$$Q_p = \begin{cases} (P-E)(1-A_i) - W_m + W & \text{if } i_m \leqq i_0 + P - E \\ (P-E)(1-A_i) - W_m + W + W_m \left(1 - \dfrac{i_0 + P - E}{i_m}\right)^{1+b} & \text{if } i_m > i_0 + P - E \end{cases} \tag{12}$$

where W is the present water storage, i_0 is the present maximum storage height in a saturated area, P is precipitation, E is evapotranspiration and dW the increase in water storage after the precipitation occurs. W_m is the maximum tension water storage over the basin (in depth units) expressed as

$$W_m = \frac{i_m}{1+b}(1-A_i) \tag{13}$$

Total direct runoff Q is obtained as

$$Q = Q_i + Q_p \tag{14}$$

In Model 1 and 2, precipitation is separated into direct runoff and soil water storage as shown in Fig. 4. In these models, Q is considered to be direct runoff R_d. The soil water storage contributes to evapotranspiration and ground water R_g express as

$$R_g = k_g W \tag{15}$$

where k_g is the sub-surface runoff coefficient. In Model 2 which is the unconfined aquifer case of Model 1, the groundwater runoff generation component becomes

$$R_g = k_g W^2 \tag{16}$$

The total runoff R is expressed as

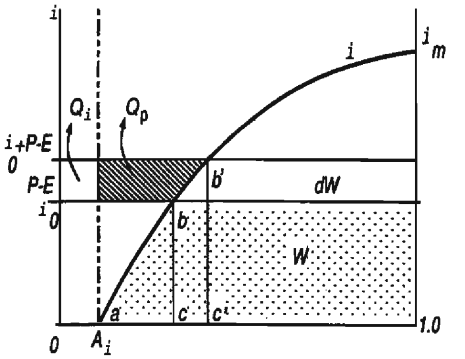

Fig. 3. The distribution of soil water storage capacity at any point.

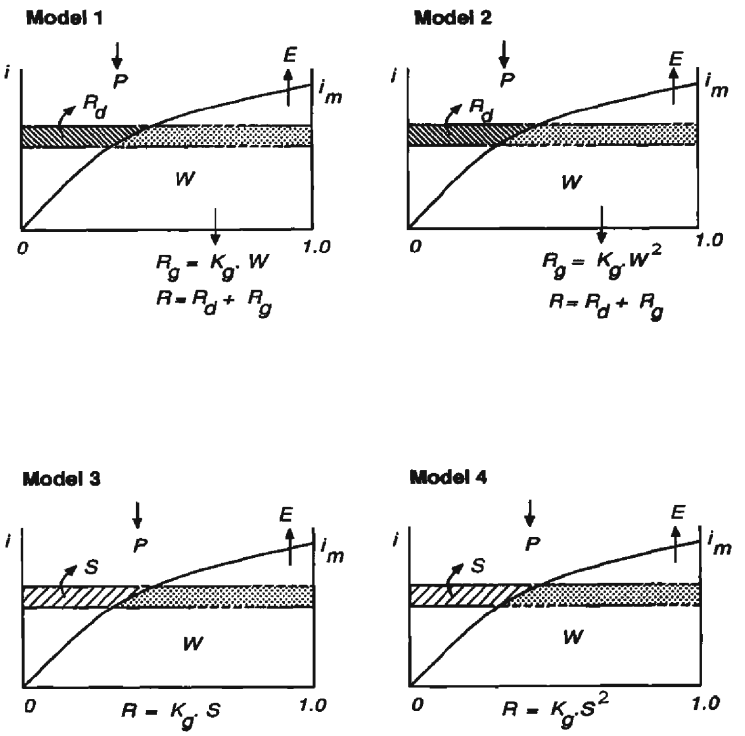

Fig. 4. The Four Models in Simple Diagrams.

$$R = R_d + R_g \tag{17}$$

For a water balance model linked with a meteorological model, it is important that the model clearly indicate the amount of water evapotranspirated and infiltrated into the ground adding to the ground water. The concept of W in Model 1 and 2 is ambiguous because soil water storage does not separate into free and tension water storage. Therefore, in Model 3 and 4, W is considered to be only tension water storage and Q is considered to be added to ground water storage S. The form of model description is similar to the VIC model, but the concept of runoff generation mechanism is quite different. S becomes ground water storage after the tension water storage reaches it's capacity at that point. In Model 3 the runoff is expressed as

$$R = k_g S \tag{18}$$

The runoff component in Model 4, which is the unconfined aquifer version of Model 3, is of the following form,

$$R = k_g S^2 \tag{19}$$

2.4 Energy Balance Method to Compute Evapotranspiration

The pan evaporation data is not always available. The Energy Balance approach was adopted to compute hourly evapotranspiration (Kondo, 1994 and Brutsaert, 1982). The procedure goes as follows:

The net radiation R_n is given by

$$R_n = S\downarrow - S\uparrow + L\downarrow - L\uparrow \tag{20}$$

where $S\downarrow$, $S\uparrow$, $L\downarrow$ and $L\uparrow$ are incoming and outgoing short wave and long wave radiation, respectively. Further,

$$R_n = R\downarrow - \varepsilon\sigma T s^4 \tag{21}$$

$R\downarrow$ consists of two components, $R\downarrow = (1-\alpha)S\downarrow + L\downarrow$ where α is the surface albedo. Short wave radiation is computed as follows

$$S_d = \begin{cases} S_{0d}\, c & \text{if} \quad \dfrac{N}{N_0} = 0 \\ S_{0d}\left(a + b\dfrac{N}{N_0}\right) & \text{if} \quad 0 < \dfrac{N}{N_0} < 1 \end{cases} \tag{22}$$

where N and N_0 ($=2H/0.2618$) represent the actual number of hours of bright sunshine, the number of daylight hours, and a, b and c are constant values which depend on the type of sunshine recorder. Here $a=0.511$, $b=0.244$, $c=0.118$. S_{0d} is computed as follows,

$$S_{0d} = \frac{I_0}{\pi}\left[\frac{d_0}{d}\right]^2 (H \sin\phi \sin\delta + \cos\phi \cos\delta \sin H) \tag{23}$$

$$H = \cos^{-1}(-\tan\phi \tan\delta)$$

$$\left[\frac{d_0}{d}\right]^2 = 1.00011 + 0.034221 \cos\eta + 0.00128 \sin\eta + 0.000719 \cos 2\eta + 0.000077 \sin 2\eta$$

$$\delta = \sin^{-1}(0.398 \sin a_2)$$

$$a_2 = 4.871 + \eta + 0.033 \sin\eta$$

$$\eta = 2\pi . a_i / 365$$

$$a_i = 30.36(month - 1) + iday$$

where *iday* is day of the month, I_0 (solar constant) $=1365\ \mathrm{Wm}^{-2}$, and ϕ is the latitude. The long wave downward radiation is computed from,

$$L\downarrow = \sigma T^4\left[1 - \left(1 - \frac{L_{df}}{\sigma T^4}\right)\cdot C\right] \tag{24}$$

$$C = \begin{cases} 0.2235 & \text{if} \dfrac{N}{N_0} = 0 \\ 0.826\left(\dfrac{N}{N_0}\right)^3 - 1.234\left(\dfrac{N}{N_0}\right)^2 + 1.135\left(\dfrac{N}{N_0}\right) + 0.298 & \text{if} \ 0 < \dfrac{N}{N_0} < 1 \end{cases} \tag{25}$$

where, C is the cloudiness factor and L_{df} represents the daily mean long-wave-downward radiation in clear sky conditions. We have used the Ångström-Limke equation for L_{df}, viz., $\frac{L_{df}}{\sigma T^4}=0.806-0.236\times 10^{-0.052e}$, here e is vapor pressure and T is the air temperature. At the surface, R_n is divided into sensible heat, H, latent heat λE (E is water vapor flux, λ is the latent heat of evaporation=2500), and heat storage G.

$$R_n=H+\lambda E+G \tag{26}$$

$$H=C_p\cdot\rho\cdot C_H\cdot u\cdot(T_s-T) \tag{27}$$

where $C_p=1005$ (J Kg^{-1} K^{-1}), the specific heat of the air, $\rho=1.293$ ($\simeq 1.2$ Kg m^{-3}), the density of the air, C_H the Bulk constant, T is air temperature and T_s is surface temperature. Here we have set C_H as 0.005. Latent heat λE is expressed as,

$$\lambda E=\lambda\cdot\rho\cdot\beta\cdot C_H\cdot u\cdot(q_{sat}(T_s)-q) \tag{28}$$

where $q_{sat}(T_s)$ is the saturation specific humidity at temperature T_s (^0C), u the mean wind speed (m/s), q the mean specific humidity and β the surface moisture availability, taken here as 0.3 which is good for forests. Heat storage $G=0$ because the study area is more than 70% forest.

From Equations (21), (26), (27), and (28), we get the following function of T_s (Equation (29)), which could be solved by the Newton-Raphson method to get E from Equation (28).

$$\varepsilon\cdot\sigma\cdot Ts^4+C_p\cdot\rho\cdot C_H\cdot u\cdot(T_s-T)+\frac{C_p}{\gamma}\cdot\rho\cdot\beta\cdot C_H\cdot u\cdot(e_{sat}(T_s)-e)-R\downarrow=0 \tag{29}$$

3. Study Area And Data Used

Two different sized sub-basins of the Yodo River catchment (Fig. 8) of Japan were identified for this study. One is referred to here as Shimagahara (525 Km^2) which is located in the south-east of the Yodo River catchment with the Shimagahara discharge station situated at the outlet point. The other, the larger one, which is the major part of the Yodo River catchment, is being called Yahata (1,600 Km^2), and covers Shimagahara also. Both these sub-basins have quite similar topography, soil moisture condition, land use and land cover, i.e., mostly forest and rice fields. In Yahata, the mean rainfall of 19 raingauge stations has been computed and the discharge time series data recorded at Yahata discharge recording station were used. In Shimagahara, the mean rainfall value of 6 precipitation recording stations has been computed and the discharge time series data recorded at Shimagahara discharge recording station were used. Both the sub-basins are almost always wet. Discharge and precipitation data were obtained from the Ministry of Construction. AMeDAS (Automated Meteorological Data Acquisition System) data for the sunshine hours, temperature, wind velocity and the vapor pressure were used.

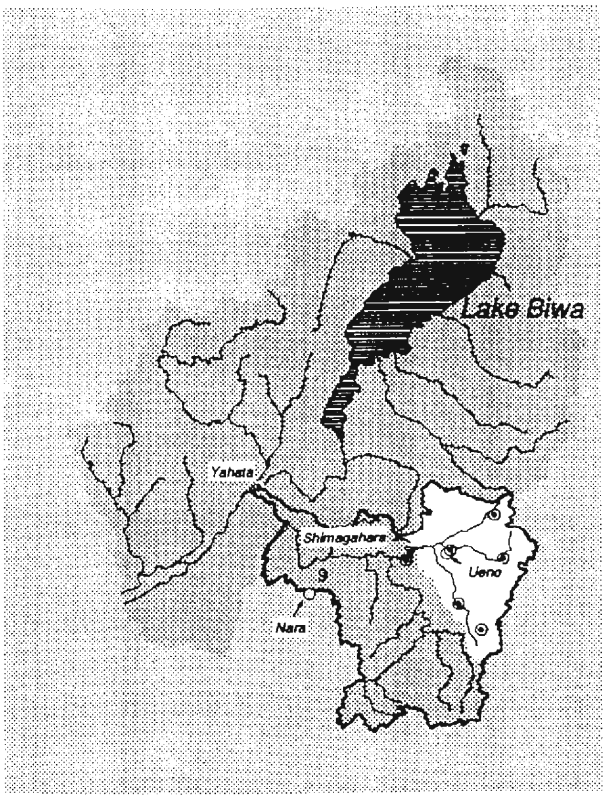

Fig. 5. Location of two sub-basins.

4. Model Performance

Using each of the four models described above, the best combination of model parameters, i.e., the shape parameter of the soil water storage curve b, the sub-surface runoff parameter k_g, and the maximum storage capacity W_m, was estimated using the time series of the year 1991. For the purpose of comparision of the performances of the VIC model and the other three models, the value of m in Equation (3) has been fixed to two. The optimization procedure based on step-size search technique has been adopted, as this procedure avoids any interaction among the parameters. However, one should first adopt a coarse step-size to identify the probable optimized parameters and then adopt a finer step-size to identify more refined values. The optimized parameters should not be identified on the boundary range of different parameters. If the optimized value of a parameter is found to be on the given boundary range of that parameter, then the boundary range of that parameter should be increased and the optimized value should be identified for that parameter again. In the present case, for the purpose of reaching at the best solution, the three parameters are searched within the following

ranges:

$$0<b\leq 2.0,\ 110\leq W_m\leq 350 \text{ (mm) and } 0.000001\leq k_g\leq 0.3.$$

The goodness of the fit has been judged based on three different criteria for the simple reason of comparison. There are instances when a particular model is good using one criterion but does not come up as good using the other criterion. The three criteria are as follows,

$$\textit{criterion } 1=\frac{|\Sigma Q_c-\Sigma Q_o|}{\Sigma Q_o} \tag{30}$$

$$\textit{criterion } 2=\Sigma\frac{|Q_c-Q_o|}{Q_o} \tag{31}$$

$$\textit{criterion } 3=1-\frac{\Sigma (Q_o-Q_c)^2}{\Sigma (Q_o-Q_m)^2} \tag{32}$$

Here Q_o is observed discharge, Q_c is computed discharge, Q_m is yearly mean discharge and *criterion* 3 is the Nash and Sutcliffe coefficient. For a perfect simulation, *criterion* 1 and *criterion* 2 should be zero and *criterion* 3 equal to one (or 100%).

Having estimated the best values of parameters for both the sub-basins, Yahata and Shimagahara separately, the validation tests are made on the year 1988 time series. The validation has been done for each best set of three parameters, i.e., best fit of *criterion* 1, *criterion* 2 and *criterion* 3, respectively.

5. Results and Discussion

Runoff simulations done with Model 1 (Figs 6–9), Model 2 (Figs 10–13), Model 3 (Figs 14–17) and Model 4 (Figs 18–21) present a comparative study in the Shimagahara sub-basin. The plots for Yahata could not be given here due to limited space. The estimated shape parameter of the soil water storage curve b, the groundwater runoff coefficient k_g, and the maximum storage capacity W_m at Shimagahara, for the year 1991 are given in Table 1 and the results of validated simulations using all three sets of parameters is given in Table 2. Similarly, the estimated parameters at Yahata have been compiled in Table 3 and the results of validated simulations in Table 4. The values of three criteria are given in percentages. We obtained three sets of estimated best fit parameters for three criteria. Using each set of parameters we have computed the values for all the three criteria, obtaining six validated simulations for each basin including hourly and daily time series case.

Results in Table 1 (Shimagahara) suggest that *criterion* 1 brings out Model 3 as the best for both daily and hourly cases, *criterion* 2 prefers Model 1 for hourly and Model 2 for daily time series is best, but according to *criterion* 3, Model 4 is best for both daily and hourly cases. Model 3 is second best in the hourly case (*criterion* 3). The interesting part of this analysis is the validation of estimated parameters. Table 2 recommends Model 4 as best in two out of a total of six cases and second best, by a small margin, in the remaining four cases. Another point to be noticed is the poor validation by Model 1 and Model 2 using *criterion* 3.

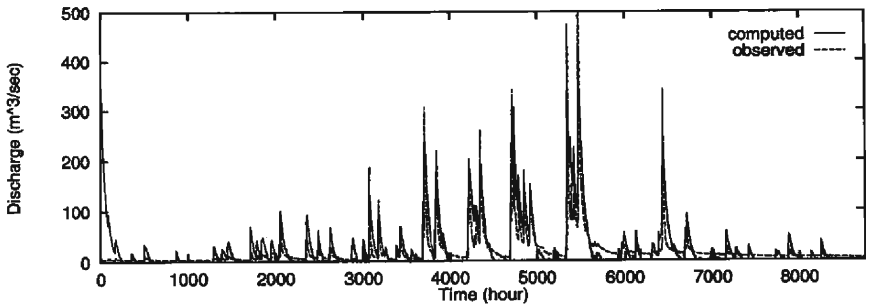

Fig. 6. Validated hourly hydrograph using Model 1 (1988).

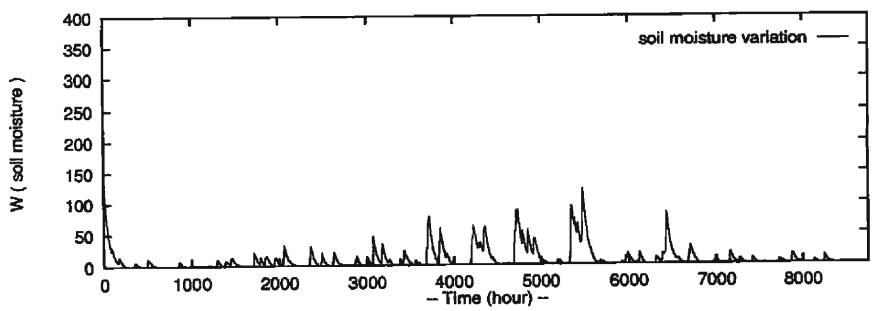

Fig. 7. Validated hourly soil water profile using Model 1 (1988).

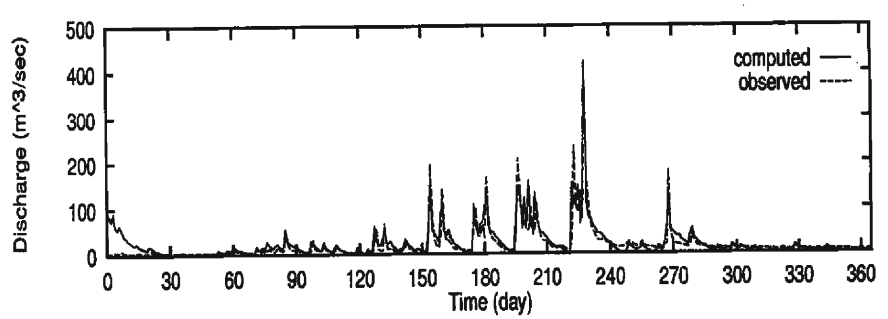

Fig. 8. Validated daily hydrograph using Model 1 (1988).

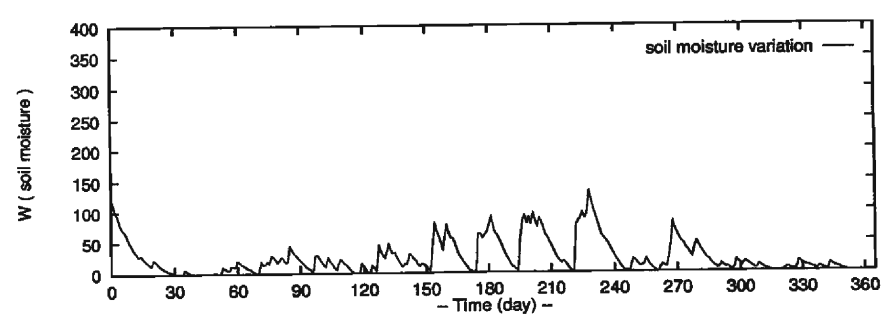

Fig. 9. Validated daily soil water profile using Model 1 (1988).

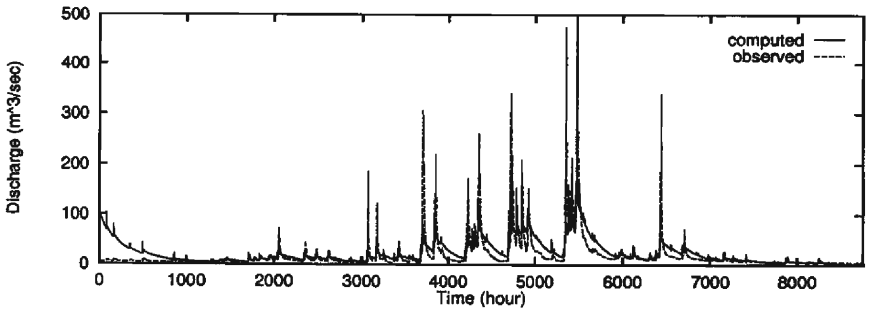

Fig. 10. Validated hourly hydrograph using Model 2 (1988).

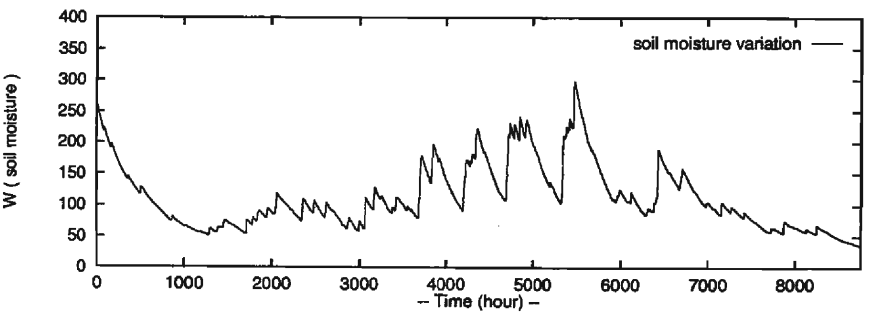

Fig. 11. Validated hourly soil water profile using Model 2 (1988).

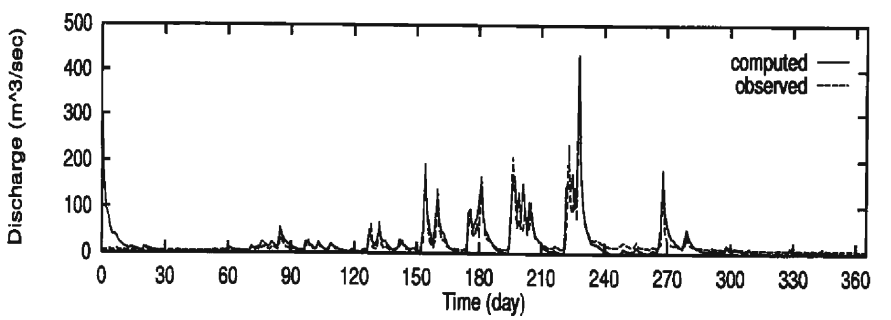

Fig. 12. Validated daily hydrograph using Model 2 (1988).

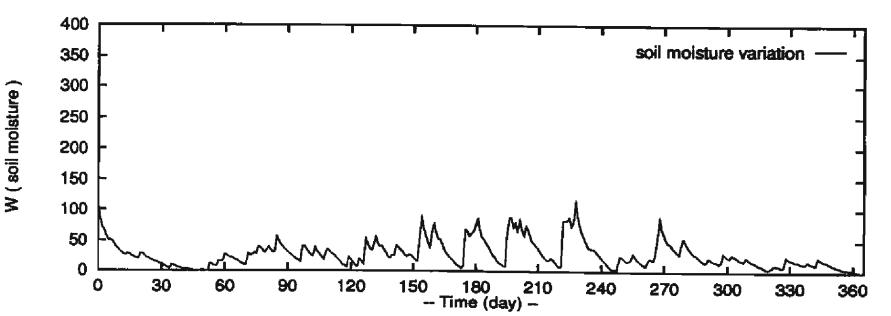

Fig. 13. Validated daily soil water profile using Model 2 (1988).

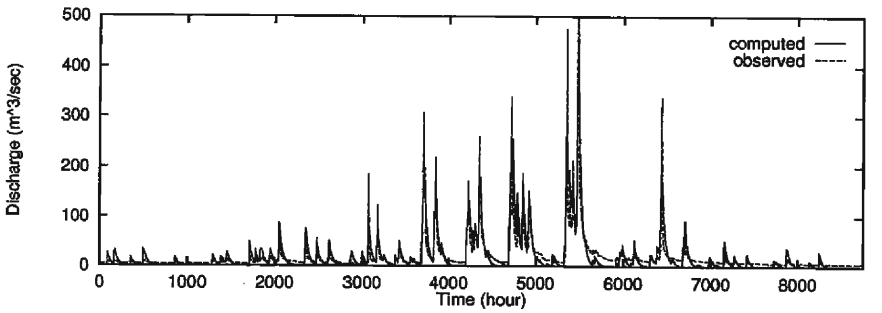

Fig. 14. Validated hourly hydrograph using Model 3 (1988).

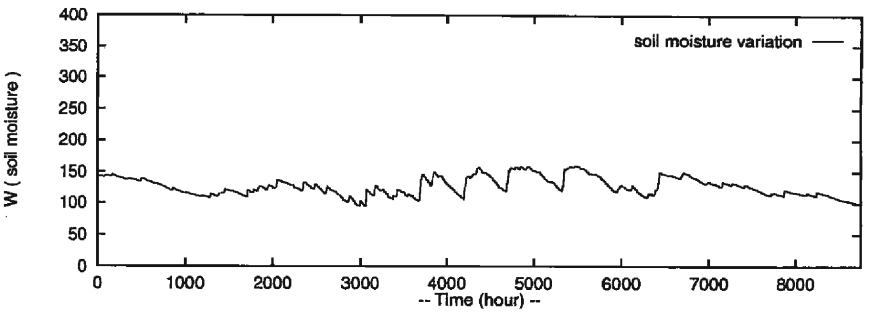

Fig. 15. Validated hourly soil water profile using Model 3 (1988).

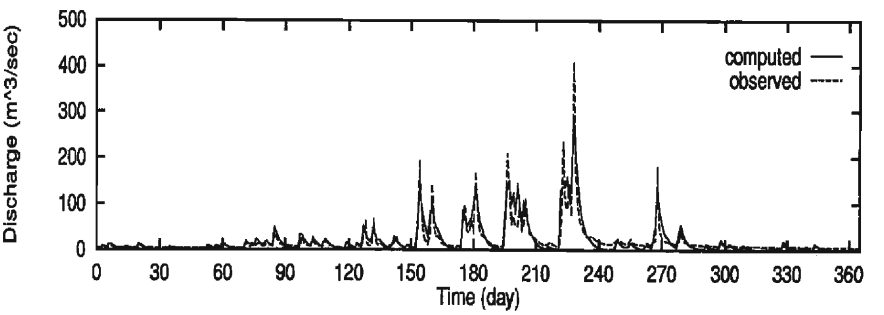

Fig. 16. Validated daily hydrograph using Model 3 (1988).

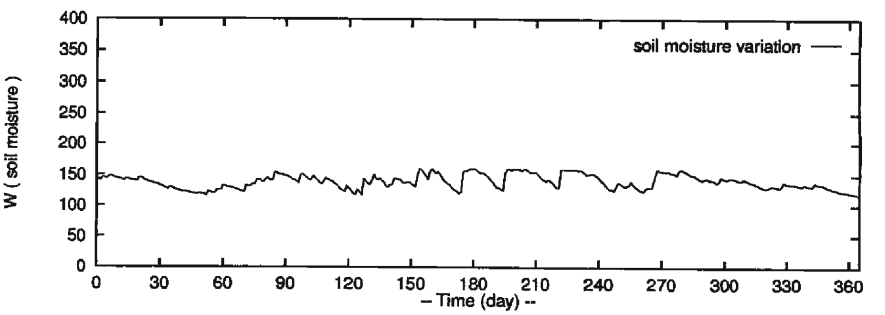

Fig. 17. Validated daily soil water profile using Model 3 (1988).

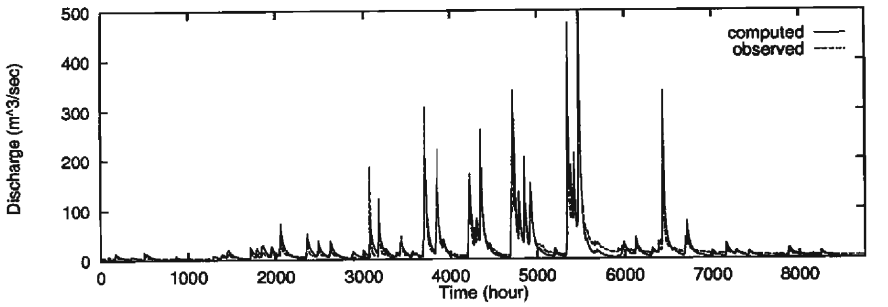

Fig. 18. Validated hourly hydrograph using Model 4 (1988).

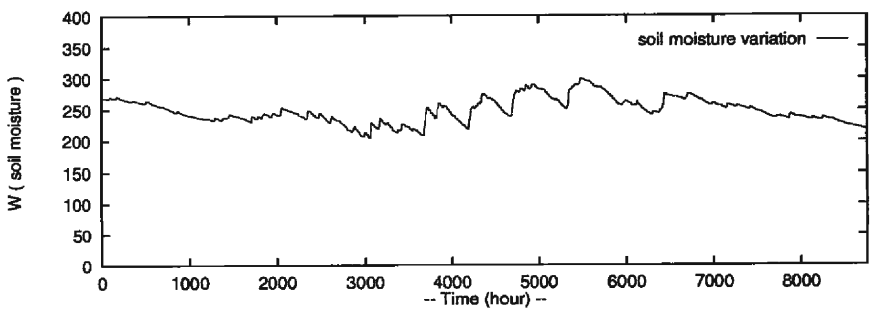

Fig. 19. Validated hourly tension water profile using Model 4 (1988).

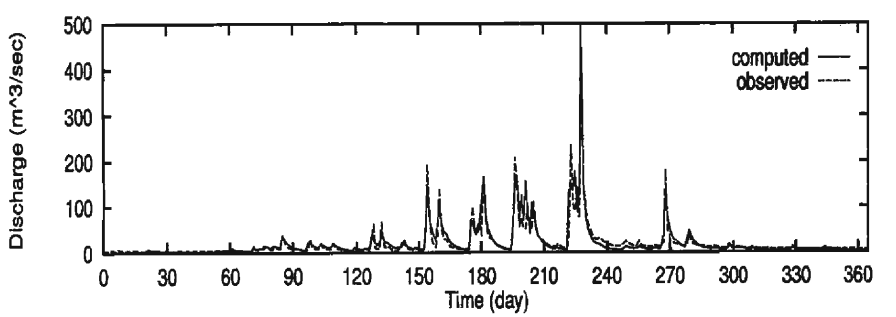

Fig. 20. Validated daily hydrograph using Model 4 (1988).

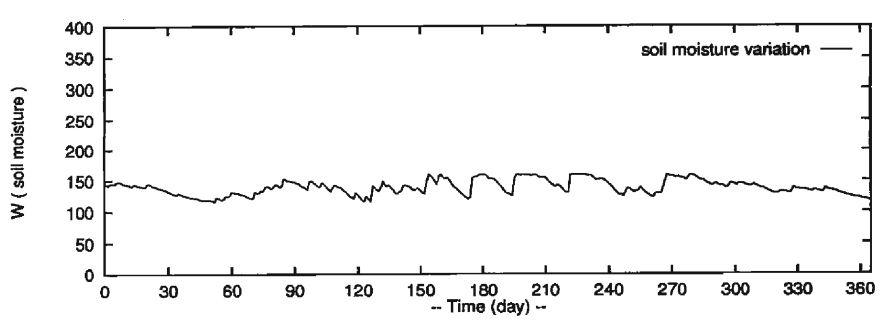

Fig. 21. Validated daily tension water profile using Model 4 (1988).

Table 1. Estimated Best Parameters for 1991 at Shimagahara

	Hourly				Daily			
	Model 1	Model 2	Model 3	Model 4	Model 1	Model 2	Model 3	Model 4
criterion 1 (%)	23.07	0.0041	0.00	0.0033	0.0055	0.09	0.0012	0.08
b	1.5	0.2	0.05	0.9	1.35	0.05	1.45	0.65
k_g	0.02	0.000002	0.15	0.05	0.02	0.0002	0.91	0.01
W_m (mm)	160	200	220	300	260	300	270	260
criterion 2 (%)	0.0000001	0.0000005	0.0007	0.000001	0.000061	0.000002	0.00025	0.000035
b	0.45	1.25	0.5	0.2	1.2	0.25	0.5	0.55
k_g	0.001	0.00001	0.02	0.0007	0.03	0.007	0.41	0.009
W_m	180	220	300	210	180	280	200	170
criterion 3 (%)	65.54	33.13	73.73	85.42	71.04	78.41	72.35	80.77
b	0.05	0.05	1.4	1.5	0.8	0.05	0.65	0.7
k_g	0.02	0.00001	0.03	0.0005	0.11	0.002	0.31	0.003
W_m (mm)	160	300	160	300	160	200	160	160

Table 2. Results of validated simulation for 1988 at Shimagahara

parameters estimated by	Hourly				Daily			
	Model 1	Model 2	Model 3	Model 4	Model 1	Model 2	Model 3	Model 4
criterion 1 (%)	23.63	2.9	0.17	1.8	7.42	8.01	1.58	4.74
criterion 2 (%)	0.0031	0.0041	0.004	0.005	0.091	0.104	0.12	0.084
criterion 3 (%)	53.61	−7.15	81.97	88.41	76.12	−700.29	81.10	80.83

Table 3. Estimated Best Parameters for 1991 at Yahata

	Hourly				Daily			
	Model 1	Model 2	Model 3	Model 4	Model 1	Model 2	Model 3	Model 4
criterion 1 (%)	27.73	29.62	12.35	0.51	50.21	28.52	16.46	18.27
b	0.05	0.05	0.05	1.5	0.05	0.05	0.05	1.5
k_g	0.000002	0.000002	0.001	0.000002	0.12	0.00002	0.03	0.00002
W_m (mm)	300	210	160	160	160	300	160	160
criterion 2 (%)	0.000001	0.000003	0.008	0.0000001	0.27	0.000001	0.126	0.000024
b	0.4	1.35	1.5	0.95	0.05	1.3	0.8	0.45
k_g	0.0004	0.000009	0.001	0.0008	0.00002	0.0002	0.03	0.01
W_m (mm)	270	190	300	240	160	240	300	210
criterion 3 (%)	46.18	3.61	58.08	65.80	98.92	61.45	59.61	62.33
b	0.05	0.05	0.7	1.5	1.5	0.05	0.55	1.5
k_g	0.007	0.000004	0.01	0.0002	0.19	0.001	0.19	0.002
W_m (mm)	300	300	300	300	160	300	300	300

Table 4. Results of validated simulation for 1988 at Yahata

parameters estimated by	Hourly				Daily			
	Model 1	Model 2	Model 3	Model 4	Model 1	Model 2	Model 3	Model 4
criterion 1 (%)	0.98	3.74	0.15	5.92	14.14	3.66	1.35	13.04
criterion 2 (%)	0.002	0.0033	0.001	0.003	0.14	0.068	0.019	0.068
criterion 3 (%)	17.74	20.73	62.94	71.33	25.62	2.03	71.25	74.34

Similar trends can be noticed in the Yahata results. Referring to Table 3, we can see that Model 4 performs best in all hourly cases, while Model 3 stands next to that. However, for daily time series, Model 4 is second best in all three criteria, whereas the best is different in each case, and that is Model 3, Model 2 and Model 1, respectively. Validation of these estimated parameters is again in the favour of Model 4 with two (both *criterion* 3) out of six as best and two out of the remaining four as next best. Model 3 performs best in four cases and is next best in the remaining two. Parameters estimated by *criterion* 1 and *criterion* 2 give the impression that Model 3 is better than Model 4 (Table 2 and Table 4). Overall the value of *criterion* 3 indicates that Model 3 and Model 4 are better than Model 1 and Model 2. In the entire experiment, there are only two instances in the estimation part when Model 4 was neither the best nor next best, viz., (i) at Shimagahara, daily time series case for *criterion* 1 and (ii) hourly time series case for *criterion* 2. Interestingly, at Yahata, it is the validation part when Model 4 performs third best for both hourly and daily time series using *criterion* 1. It is clear that out of a total of 24 cases of estimation and validation it is Model 4 in twenty cases that performs either best or second best (in this case mostly Model 3 is best) with a more realistic soil water storage profile (Figs. 15, 17, 19 and Fig. 21).

Please refer to Fig. 7 and Fig. 9 to note that using Model 1, the soil water storage profile is not realistic for a humid region. Model 2 generates better profiles (Fig. 11) for hourly time series but a non-realistic plot (Fig. 13) for daily time series. The soil water storage profiles show more realistic behavior in all the cases of Model 3 and 4. Close observation of the results shows that Model 3 and 4 perform best among the four models.

6. Sensitivity of Model Parameters

The three parameters, soil water storage distribution shape parameter b, maximum tension water storage capacity W_m and groundwater runoff coefficient k_g, varied depending on various factors. To study the variation in each of them, computer runs were made using *criterion* 3 (explained variance), as the deciding factor to choose the best fit for each value of a parameter separately. Model 4 was chosen for this purpose. In this way, a time series was obtained and the results of senstivity of parameters were plotted as shown in Figs (22)-(27) for both daily and hourly data cases, at Shimagahara.

Fig. 28 makes it easy to understand the phenomenon of sensitivity in the parameters. When an area was almost saturated as illustrated in Fig. 28(a), b became in-

sensitive because portions $A1$, $A2$ and $A3$ were almost equal. Similarly, W_m also became insensitive in an almost saturated area. In such cases, even the bucket model case ($b=0$) did not alter the estimated value of W_m. Whereas in relatively dry conditions, as illustrated in Fig. 28(b), the shape parameter became sensitive as did W_m. Areas $A1$, $A2$ and $A3$ were very much different from each other in this situation.

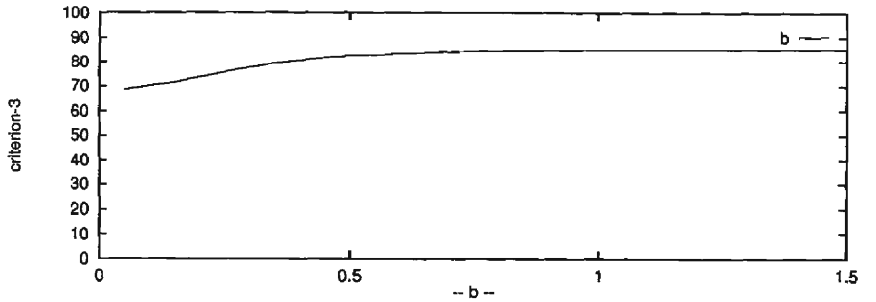

Fig. 22. Sensitivity of b using Model 4 for the hourly case (1991).

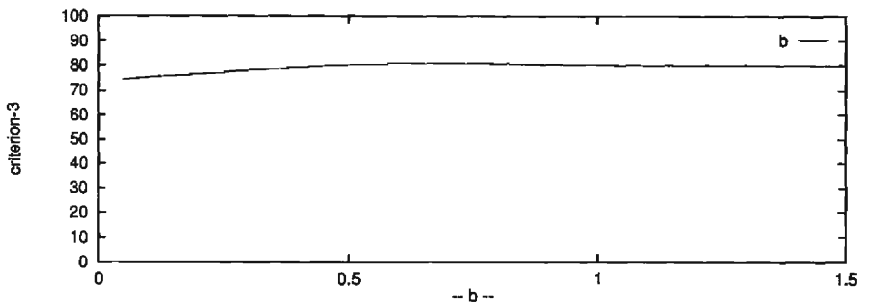

Fig. 23. Sensitivity of b using Model 4 for the daily case (1991).

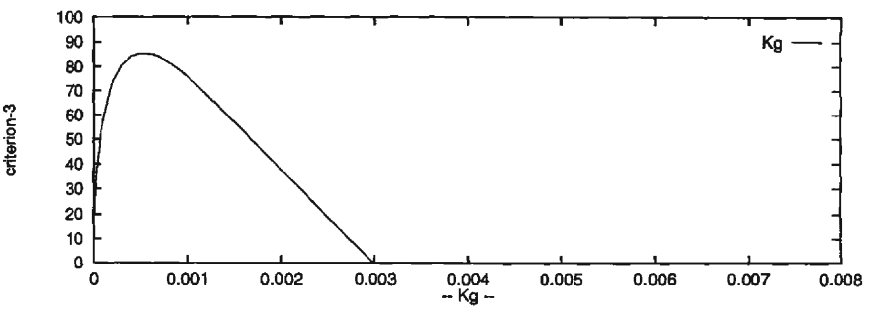

Fig. 24. Sensitivity of k_g using Model 4 for the hourly case (1991).

The effect of time and areal scale on the parameters of the models was examined and the findings compiled in Table 5. Clearly, W_m and b were unaffected, while k_g increased with an increase in time interval of the time series. When the area of the basin increased k_g decreased. Other parameters did not vary significantly.

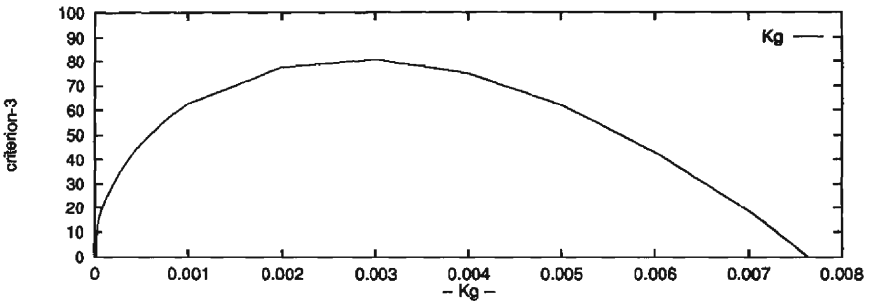

Fig. 25. Sensitivity of k_g using Model 4 for the daily case (1991).

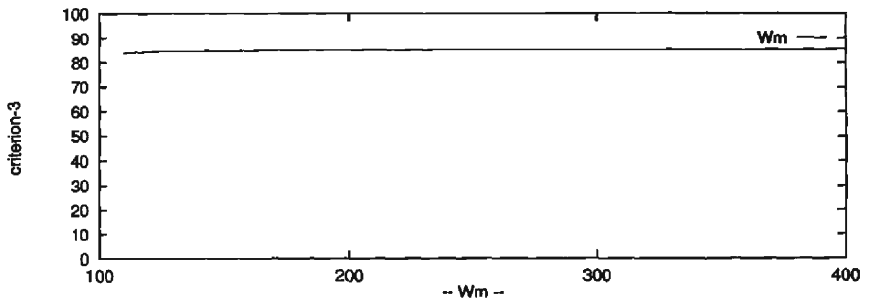

Fig. 26. Sensitivity of W_m using Model 4 for the hourly case (1991).

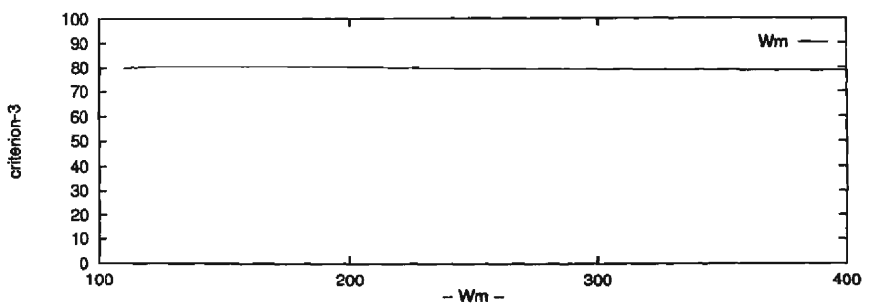

Fig. 27. Sensitivity of W_m using Model 4 for the daily case (1991).

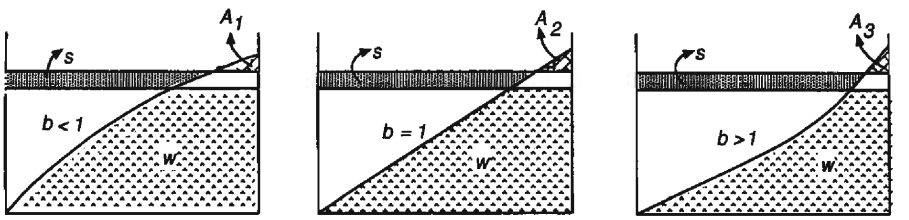

(a): nearly saturated area

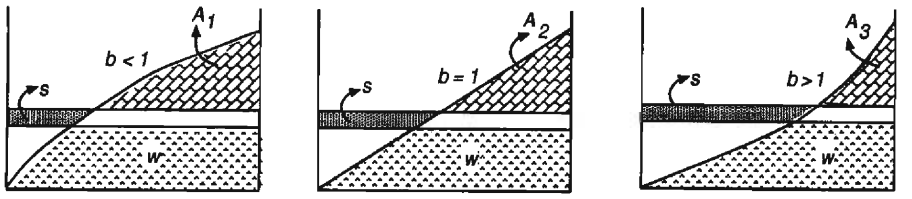

(b): unsaturated area

Fig. 28. Explanation of sensitivity of b and k_g depending on W.

Table 5. Time and Area Effect on Parameters for 1991

time interval	Shimagahara				Yahata			
	b	k_g	W_m	*criterion* 3	b	k_g	W_m	*criterion* 3
1 hour	1.5	0.0005	300	85%	1.5	0.0002	300	66%
4 hour	1.5	0.002	300	86%	1.5	0.0007	300	68%
6 hour	1.5	0.003	300	86%	1.5	0.001	300	70%
10 hour	1.5	0.005	300	85%	1.5	0.002	300	71%
12 hour	1.5	0.007	300	83%	1.5	0.003	300	73%
1 day	0.6	0.003	160	81%	1.5	0.002	300	62%
2 day	1.5	0.005	300	78%	1.5	0.004	300	60%
3 day	0.6	0.01	290	80%	1.5	0.006	300	63%
4 day	1.5	0.01	300	72%	1.5	0.007	300	46%
6 day	1.5	0.03	300	82%	1.5	0.02	300	64%

7. Application of developed models to a sub-basin of Thailand

In order to study the four models described in the previous sections, for other regions different from the Japanese river basins, in terms of climate and other natural conditions, a study basin of 1335 km^2 was identified in the Ping River catchment area. The daily discharge and rainfall observations recorded at Chiang Dao were used. Following the same procedure as explained in Section 4., the year 1991 was selected for estimation of model parameters. Having estimated the model parameters, the validation test based on the year 1987 time series data was carried out. This selection of valida-

tion time series was done from two stand points, that is, it should be different from the time series used for estimation of parameters of the model, and there should not be many missing values in the data. To identify the best combination of the three model parameters, we tried the following ranges: $0<b\leq 1.5$, $50\leq W_m\leq 400$ (mm) and $0.00001\leq k_g\leq 0.5$. The results are compiled in Table 6, which clearly shows that although Models 3 and 4 performed better than Models 1 and 2, they still left much to be desired. Due to limited space other hydrographs could not be presented here. Fig. 29 and Fig. 30 illustrate the validated runoff hydrographs using Models 3 and 4, respectively. One can notice from these hydrographs that Model 4 provided a better simulation over the one produced by Model 3. In particular the low flow stretch and the last peak in Fig. 30 better matches the observed hydrograph. Sensitivity analysis conducted on Model 4 shows that all three parameters vary quite substantially. As illustrated in Fig.

Table 6. Estimated and Validated Results at Chiang Dao.

Model	b	k_g	W_m	criterion 3	
				estimation	*validation*
1	*0.02*	*0.02*	*400*	*30%*	39%
2	0.3	0.0001	400	27%	35%
3	1.1	0.06	320	66%	49%
4	1.0	0.0006	320	67%	60%

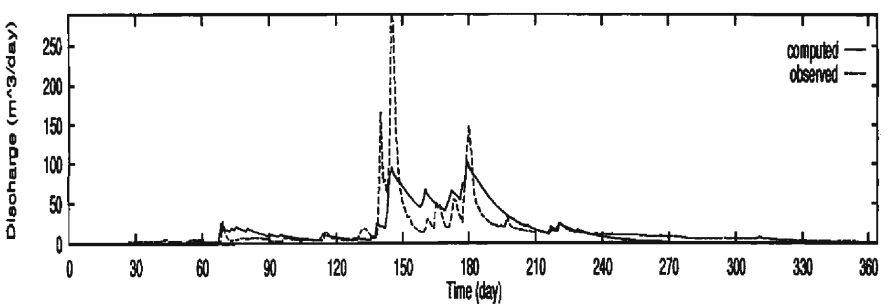

Fig. 29. Thailand: Validated Hydrograph obtained from Model 3 for 1987.

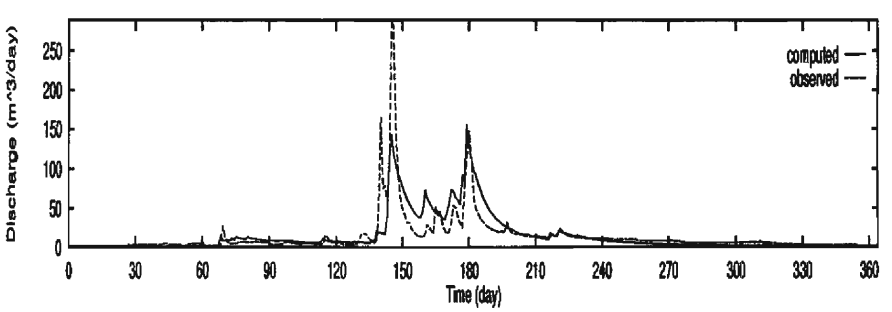

Fig. 30. Thailand: Validated Hydrograph obtained from Model 4 for 1987.

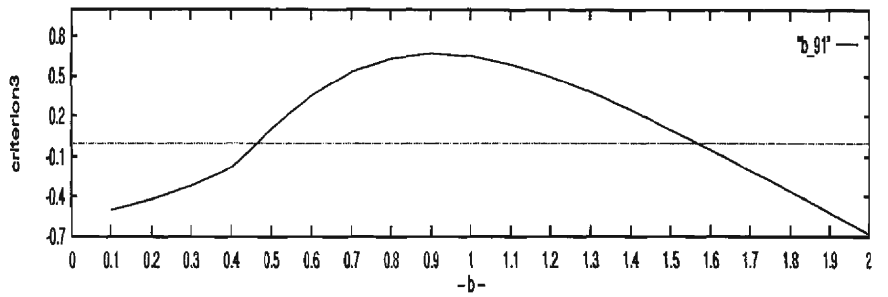

Fig. 31. Thailand: Variation in b using Model 4–1991.

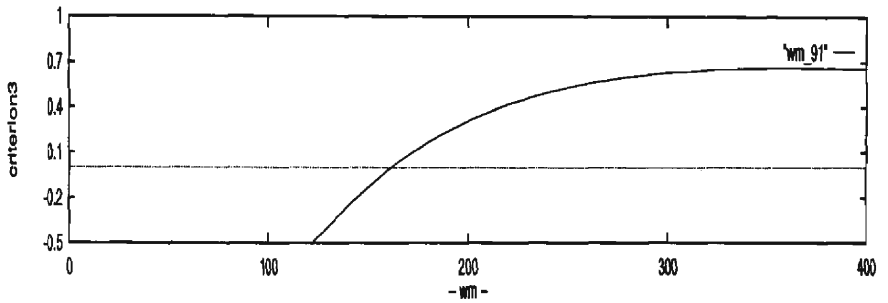

Fig. 32. Thailand: Variation in W_m using Model 4–1991.

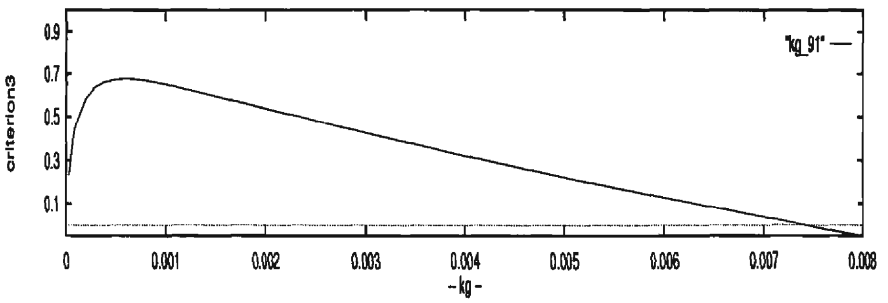

Fig. 33. Thailand: Variation in k_g using Model 4–1991.

31, Fig. 32 and Fig. 33, change in soil water distribution shape parameter b, in the order of 0.1 each step-size, alters the value of *criterion* 3 considerably. A similar pattern can be noticed in the case of k_g, but for W_m, once the soil is saturated, increase in W_m does not affect *criterion* 3 much. This phenomenon confirms that due to the geographical and meteorological conditions, runoff simulation in this Thai river sub-basin is not similar to that of the Japanese river sub-basin.

8. Concluding Remarks

In this paper, we have proposed a general expression for spatial soil water storage

capacity distribution and compared the performances of four kinds of water balance models. As discussed above and illustrated through the tables and figures, we can summarize our analysis findings as follows:

1. Although the generalization suggested in Section 2.2 increases the parameters in the original Xinanjiang model, it would make the model much more flexible and provide better simulations.
2. The ground water runoff generation concept adopted in Model 3 and 4, i.e., the outflow runoff Q is added to ground water storage S and the ground water runoff component is a linear or non-linear function of S, seems to apply better than the concept adopted in Model 1 and 2, i.e., the ground water runoff component is taken as a linear or non-linear function of soil water storage W.
3. Model 3 and 4 provide a more realistic water storage variation pattern, better simulated runoff and consistent results.
4. In case of the Ping River basin of Thailand, a similar trend in terms of performance of the four models can be noticed.
5. As far as a humid region is concerned, the parameters b and W_m become almost invariable and can be called time and area independent. Only k_g varies widely (depending on hourly or daily time series data), as revealed from the sensitivity analysis. With a slight change in k_g the estimated runoff could be altered considerably.
6. The Thai river basin study supports the fact that the parameters could become more sensitive in unsaturated conditions as demonstrated in Fig. 28.
7. It is clear that the model response in toropical catchment with wet and dry seasons would not be the same as in wet and humid catchments.

Acknowledgments

We are grateful to the Yodogawa Work Office, Kinki Regional Construction Bureau, Ministry of Construction, Japan, and the Royal Irrigation Department of Thailand for providing the data sets. I wish to thank Mr. Akira Fujita for his valuable help throughout. A part of this work was supported by the Grant-in-Aid for Scientific Research 'Hydrological Environment in Southeast Monsoon Asia' and 'Development of Macroscale Hydrological Model Considering the Time and Space Distribution of Hydrological Variables' (representative Professor, K. Musiake, Tokyo Univ.) of the Ministry of Education, Science and Culture in Japan.

References

Brutsaert, W. (1982): Evaporation into the Atmosphere Theory, History, and Applications, Kluwer Academic Publishers.

Dümenil, L. and E. Todini (1992): A rainfall-runoff scheme for use in the Hamburg climate model, Advances in Theoretical Hydrology, A Tribune to James Dooge, J.P. O'Kane (Ed.), 129.

Kalma, J. D., B. C. Bates and R. A. Woods (1995): Predicting Catchment-Scale Soil Moisture Status With Limited Field Measurements, Hydrological Processes, Vol. 9, 445–467.

Kondo, J. (1994): Climatology of Water Environment, Asakura Publishing Co. Ltd.

Lu, M., T. Koike and N. Hayakawa (1995): Runoff Analysis of Takatoki River using Xinanjiang Model, Proc. Annual Conference, Japan Society of Hydrology and Water Resources, 150–152.

Nirupama, Y. Tachikawa, M. Shiiba, and T. Takasao (1995): Estimation of River Discharge Using Xinanjiang Model, Annual Journal of Hydraulic Engineering, JSCE, Vol. 39, 91–96.

Takagi, F. (1966): A Study on the Recession Characteristics of Ground Water Flow, Proc. JSCE, Vol. 128, 1–11.

Sivapalan, M. and R. A. Woods (1995): Evaluation of the Effects of General Circulation Models Subgrid Variability and Patchiness of Rainfall and Soil Moisture on Land Surface Water Balance Fluxes, Hydrological Processes, Vol. 9, 697–717.

Wood, E. F., D. P. Lettenmaier and V. G. Zartarian (1992): A Land-Surface Hydrology Parameterization With Subgrid Variability for General Circulation Models, J. of Geophy. Res., Vol. 97, No. D3, 2717–2728.

Zhao, R. J., Y. L. Zhang, L. R. Fang, X. R. Liu and Q. S. Zhang (1980): The Xinanjiang model, Hydrological Forecasting Proceedings of the Oxford Symposium, IAHS Publ., Vol. 129, 351–356.

Zhao, R. J., (1992): The Xinanjiang model applied in China, Journal of Hydrology, Vol. 135, 371–381.